THE VALENCE STATES OF 3d: TRANSITION ELEMENTS
# IN APOLLO 11 AND 12 ROCKS

ALVIN J. COHEN

University of Pittsburgh, Pennsylvania, U.S.A.

Abstract. The absorption spectra of Apollo 11 fine-grained rocks, 10017 and 10022 are due entirely to pyroxene minerals. Spectral bands due to Fe^{3+}, Fe^{2+}, Cr^{3+} and Ti^{4+} and Ti^{3+} are detected. Single crystals of olivine in rocks 12021 and 12018 show bands due to Fe^{3+}, Fe^{2+}, Cr^{3+}, Ti^{3+}, Mn^{3+}, and Mn^{2+}. Pyroxenes in the same rocks exhibit band maxima of the same cationic species as in the olivines. Spectral shifts are noted due to anisotrophy of the crystal structures.

Heating sections 10017, 10022, and 12018 from the rock interiors at 200–225 °C for 2 h caused large decreases in the spectral intensity of Fe^{3+}, Cr^{3+} and Ti^{3+}, indicating the following reaction:

$$Fe^{3+} + Cr^{3+} + Ti^{3+} \rightarrow Fe^{2+} + Cr^{2+} + Ti^{4+}$$
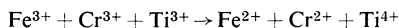
This suggests that Fe^{3+}, Cr^{3+} and (a portion of) Ti^{3+} are not in equilibrium. It is most probable that they were produced subsequent to the formation of the rocks by a combination of secondary ionization processes following cosmic ray bombardment and by trace radioactivity present in the rocks.

An orange glass, 150 μ in diam and 50 μ thick contained in brecciated rock, 10048.44, exhibited 15 identifiable absorption bands related to Fe^{2+}, Cr^{3+}, Ti^{3+}, Mn^{3+} or Mn^{2+} ions.

Plagioclase in 12021.65 has perfect transmission over the region studied. The limit of Fe^{3+} is in the order of < 1 ppm and Fe^{2+}, 1000 ppm or less in this plagioclase single crystal of dimensions 0.6 mm × 0.2 mm × 30 μ.

1. Introduction

Although Fe^{3+} and Ti^{3+} have been detected in Apollo 11 rocks by spectrophotometric (Hapke *et al.*, 1960) and by EPR techniques (Weeks *et al.*, 1970), no mechanism for their origin in lunar minerals has hitherto been suggested. The absorption spectra of lunar pyroxene and olivine crystals are reported here in detail for the first time. Due to the random orientation of these crystals, in polished sections 30 μ thick, the anisotropy of the spectra was not investigated.

A. EXPERIMENTAL

The absorption spectral data were taken using a Cary Model 14 Spectrophotometer with IR-1 Modification and a halogen lamp of variable intensity as a light source in the visible and infrared regions investigated. The spectra of the small single crystals and glass were measured using matched circular slits of 2 mm diam in sample and reference beams of the instrument. All samples investigated were approximately 30 μ thick except for the orange glass from rock 10048.44 which was approximately 50 μ thick. All single crystals measured were 2 mm or greater in diameter except the pyroxene, 12018.50 which was a grouping of several smaller crystals. The orange glass was 150 μ in diam, surrounded by an opaque matrix of the breccia in which it was embedded.

The thinness of the specimens studied precluded detection of weak *d-d* transitions of the Fe^{3+} ion. The 30 micron thickness was necessary in order to study the intense Fe^{3+} charge-transfer bands in the ultraviolet region. The Fe^{3+} band peak could not
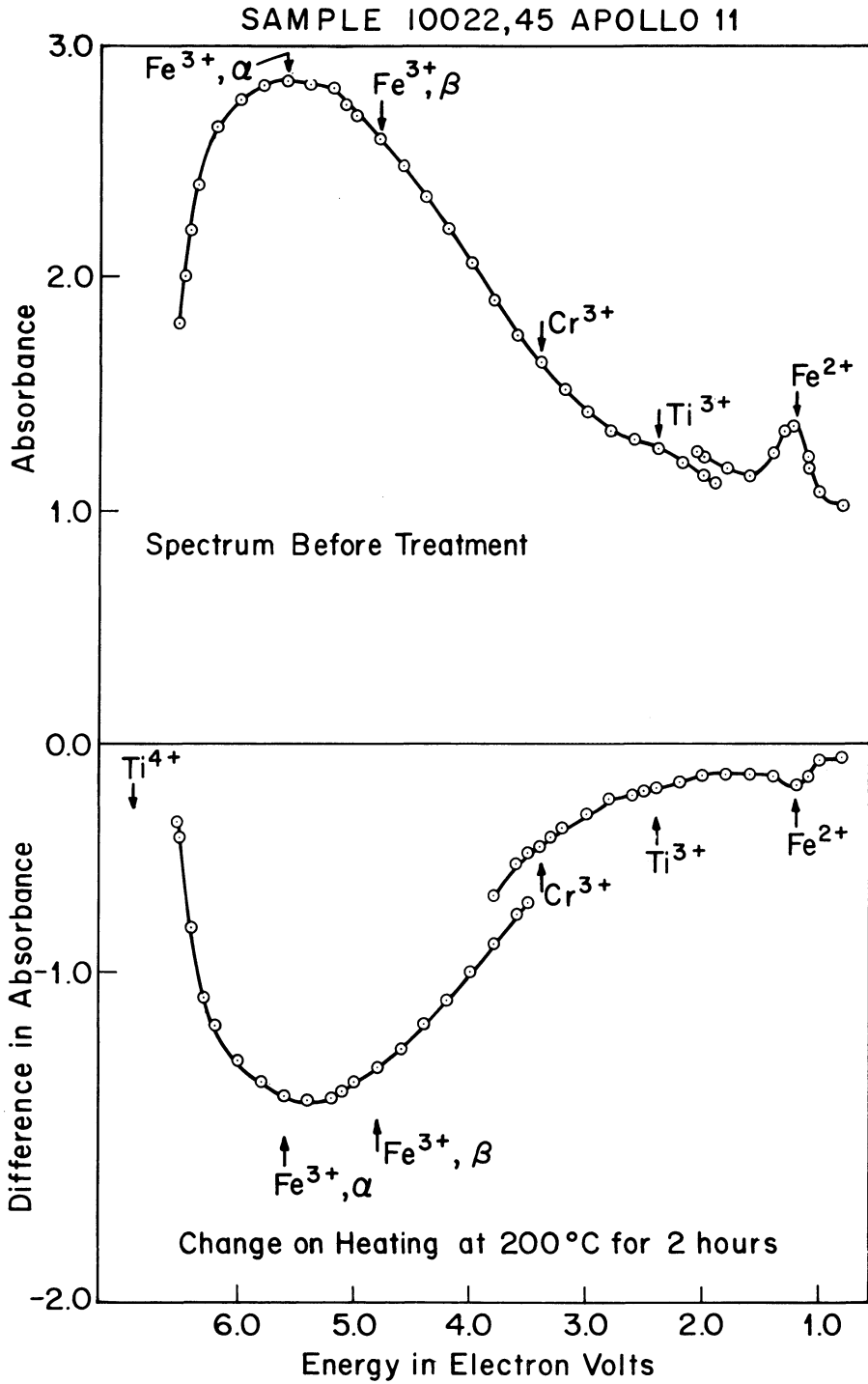
Fig. 1.

be measured in the orange glass due to the thickness of 50 μ. Screens were used in the reference beam to extend the optical density range of the spectrophotometer in order to measure the Fe^{3+} peak in all cases.

The polished sections were mounted on specially machined brass holders so that the spectrophotometer beam passed only through the sample under investigation, no other extraneous matter being present.

2. Absorption Spectra of whole Rock Before and after Heating at 200–225 °C for two Hours

The effect of heating on the absorption spectrum of a polished interior section of Apollo 11 rock, 10017 has been published earlier (Hapke *et al.*, 1970). The heating at 200 °C for 2 h followed irradiation with ultraviolet light and X-rays. After standing, the effect is similar to heating pristine 10022 or 12018 pristine interior rock. Figure 1 shows the spectrum of rock 10022.45 before heating and the change in the spectrum caused by heating at 200 °C for 2 h. The second spectrum is obtained by subtracting the spectrum taken before heating from one measured after heating. The result is a difference spectrum. Spectral bands below zero indicate a decrease in each given band appearing there. This is the result of a decrease in the specific absorbing ion causing the band. Thus one sees in Figure 1 a decrease in bands due to Fe^{3+}, Cr^{3+}, Ti^{3+} and Fe^{2+}. Rock 10022 (similarly 10017) contains little olivine but is rich in pyroxenes, plagioclase and ilmenite. The plagioclase is transparent in the region studied and the ilmenite is opaque. The absorption spectrum of this rock is due
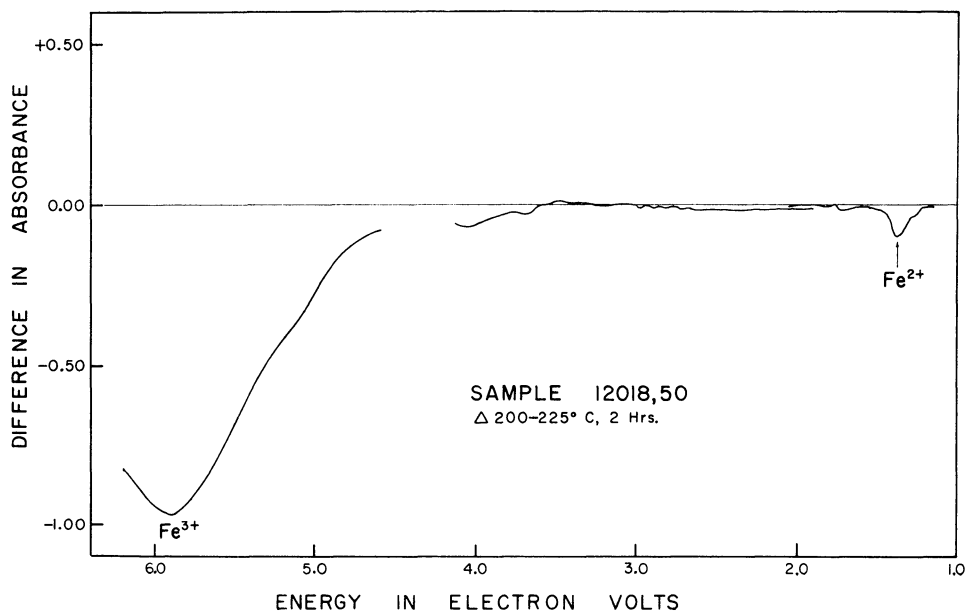

Fig. 2.

entirely to the pyroxene minerals present and changes upon heating are therefore changes in the pyroxene. The apparent decrease of the Fe^{2+} on heating is because of the interaction of neighboring Fe^{3+} and Fe^{2+}, probably across t2g orbitals. Thus decrease in the concentration of the Fe^{3+} causes an apparent decrease in the Fe^{2+} although the amount of Fe^{2+} is actually increasing slightly.

Figure 2 illustrates the difference spectrum of Apollo 12 rock 12018.50, an interior portion, upon heating at 200–225 °C for two hours. The major effects noted are decreases in Fe^{3+} and Fe^{2+} bands. This rock contains both pyroxenes and olivine and thus the difference spectrum is more complex than in the other two rocks studied. Table I summarizes the bands found to decrease upon heating at 200–225 °C in all

TABLE I

Negative difference spectra, after heating at 200–225 °C
for 2 h, all specimens approximately 30 μ thick

Absorbing ion	Peak maximum in eV		
	Apollo 11 10017	Apollo 11 10022	Apollo 12 12018
Fe^{2+}	1.1	1.3	1.28, 1.37
Ti^{3+}	–	2.4	1.72, 2.46
Cr^{3+}	3.2, 3.53	3.5	1.82, 1.94, 3.20, 3.70, 4.06
Fe^{3+}	4.5	–	–
Cr^{3+}	4.8	4.8	5.28
Fe^{3+}	5.5	5.5	5.90
Ti^{4+}	tail > 6	tail > 6	tail > 6

three rocks. The transitions to which the bands are related will be discussed when the spectra of the individual minerals are presented. Two positive bands are observed in Figure 2 at 3.35 and 3.42 eV. A band due to Mn^{2+} appears in spodumene at 3.35 eV (unpublished work) and this may be a similar transition in lunar augite. The band at 3.42 may also be due to Mn^{2+}.

The decrease of Fe^{3+}, Cr^{3+} and Ti^{3+} upon heating at relatively low temperature has been interpreted as reduction of the Fe^{3+} and Cr^{3+} accompanied by oxidation of the Ti^3 according to the following equation:

$$Fe^{3+} + Cr^{3+} + 2Ti^{3+} \rightarrow Fe^{2+} + Cr^{2+} + 2Ti^{4+}$$
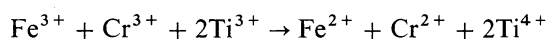
This reaction takes place in both pyroxenes and olivine as will be shown later.

An examination of the three rocks studied indicates that they have all cooled slowly. Under these conditions one expects to find the cations in the individual minerals in equilibrium. If this is true, one would not expect oxidation-reduction reactions to take place among the cations at a temperature as low as 200–225 °C. It is known that natural α- and β-radiation cause oxidation of Fe^{2+} in terrestrial minerals. β-radiation is more efficient than α-radiation. Cosmic rays are a rich source

ALVIN J. COHEN

of secondary β-rays. Therefore it is suggested that both Fe^{2+} and Cr^{2+} are oxidized by secondary radiation from cosmic rays as well as by natural radioactivity present in the lunar rocks. A Ti^{4+} ion is reduced to Ti^{3+} for each Fe^{2+} and Cr^{2+} originally present in the rock that is oxidized to Fe^{3+} and Cr^{3+}. It is suggested that a major portion of these three ionic species are produced in the pyroxene and olivine of lunar rocks after the rocks have cooled and been subjected to subsequent radiation.

The conclusion that ferric iron was produced subsequent to the cooling of the rock is strengthened by the low oxygen fugacity found in lunar rocks and by the absence of magnetite.

The probable location of the ions, being oxidized or reduced, in the mineral structure will be suggested when the individual mineral is discussed.

3. Spectra of Pyroxene in Rocks 12021 and 12018

Rock 12021 has crystals of large size compared to Apollo 11 rocks. Some pyroxene grains have zones of differing color. These colored zones consist of a core of greenish yellow pigeonite rimmed with a brown zone of augite pyroxene. (Warner, 1970). The absorption spectrum of the pyroxene single-crystal measured in rock 12021.65 was a zoned crystal as described above. The spectrum is shown in Figures 3 and 4 as a dashed curve. The absorption band maxima attributed to Fe^{2+} are listed in Table II. The Fe^{2+} spectrum consists of two d-d transitions of Fe^{2+} in M_1 sites in the structure and two d-d transitions due to Fe^{2+} in M_2 sites. The configuration of the M_1 site is that of a regular octahedron and that of the M_2 site is that of a distorted
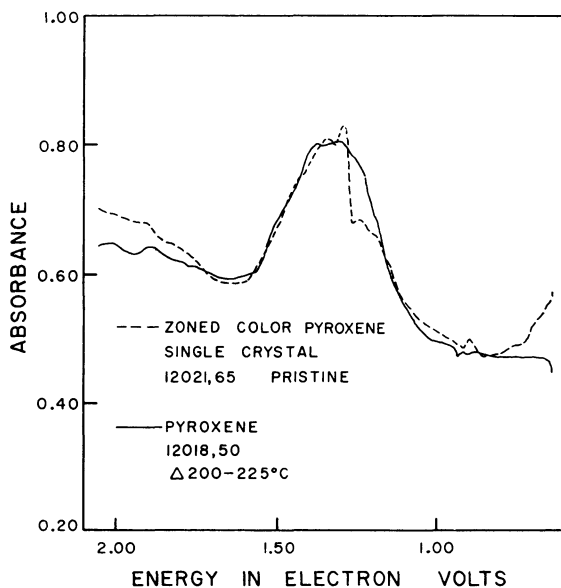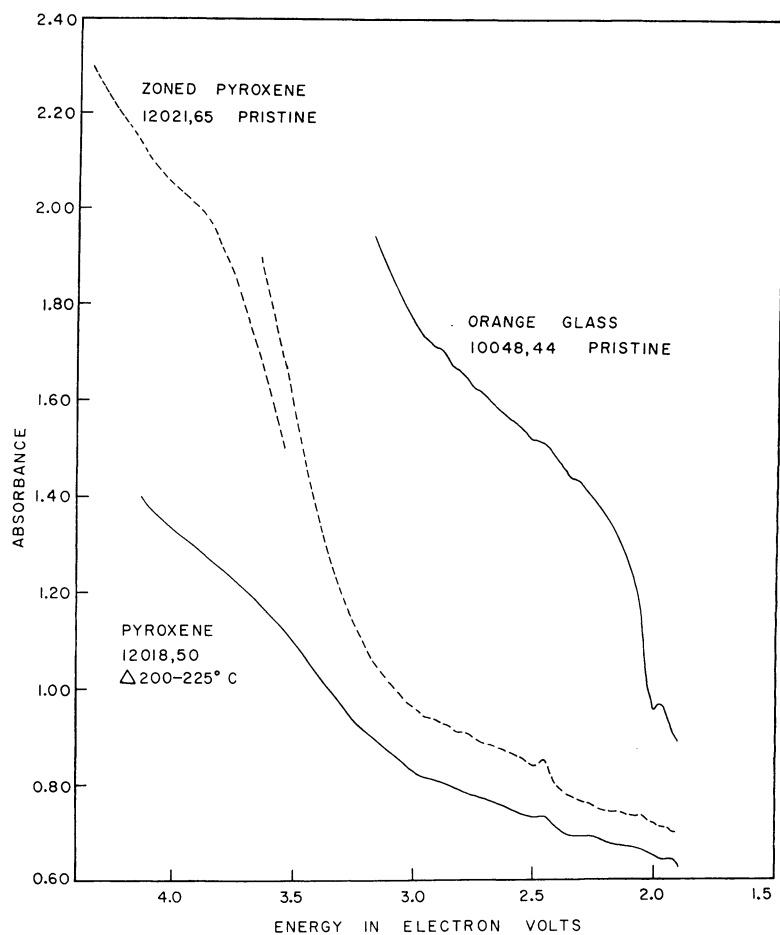

Fig. 3.

Fig. 4.

TABLE II

Ferrous absorption bands in zoned pyroxene crystal from rock 12021.65

Structural position	Band maximum in eV	Absorbance	Δ cm^{-1}
M_2–pigeonite	0.675	0.58	5 440
M_2–augite	0.75	0.49	6050
M_1–pigeonite	1.19	0.66	9 600
M_1–augite	1.24	0.68	10000
M_1–pigeonite	1.29	0.85	10405
M_2–augite	1.34	0.81	10810
M_1	1.41	0.76	11370
charge transfer ⎰ Pigeonite	1.97	0.71	15890
$Fe^{2+} \rightarrow Fe^{3+}$ ⎱ Augite	2.01	0.72	16210

polyhedron. Since one would expect the Fe^{2+} in an equivalent site in pigeonite to absorb energy at a lower value (longer wavelength) than in titanaugite, the M_1 and M_2 absorption bands are doubled (except for the M_1 transition at 1.41 eV) for transitions of Fe^{2+} in each of the two regions of the structurally-zoned pyroxene crystal. The charge-transfer band is also doubled, because of an energy-shift in the two zones of the crystal.

In the pyroxene structure one would ordinarily expect Fe^{3+} to favor M_1 positions and Fe^{2+} to favor M_2 positions. However, if the Fe^{3+} is caused by radiation damage it is not yet possible to predict whether a Fe^{2+} in an M_2 or M_1 site will be favored or whether the oxidation of Fe^{2+} to Fe^{3+} will be a random process favoring neither structural position.

Table III lists the Fe^{2+} bands in a wine-brown pyroxene in Apollo 12 rock 12018.50

TABLE III

Ferrous and ferric absorption bands in a poly-crystalline aggregate of pyroxene from rock 12018.50 after heating at 200–225 °C for 2 h

Ion	Structural position	Band maximum in eV	Absorbance	Δ cm^{-1}
Fe^{2+}	M_2	0.66	0.48	5325
Fe^{2+}	M_1	1.265	0.78	10205
Fe^{2+}	M_2	1.31	0.80	10565
Fe^{2+}	M_1	1.38	0.80	11130
Fe^{2+}	Charge transfer $Fe^{2+} \to Fe^{3+}$	1.94	0.67	15650
Fe^{3+}	Charge transfer	5.635	2.54	45450

after heating at 200–225 °C for 2 h. The pyroxene crystals in this rock are also relatively large. In the polished section studied, the best region of 2 mm diam was a clump of pyroxene crystals of the same color. The absorption spectrum of this clump of pyroxene crystals is shown in Figures 3 and 4. These crystals are of the same thickness as the zoned-crystal in rock 12021. The intensity of the absorption is almost identical in the infra-red region as shown in Figure 3. However, the Fe^{2+} spectrum is not doubled. In comparing the absorption peak positions to those listed in Table II, one cannot choose whether the polycrystalline aggregate of crystals is pigeonite or augite.

The Fe^{3+} charge transfer band is so intense in the zoned pyroxene, it could not be measured. In the pyroxene in rock 12018 after heating, the intensity of the Fe^{3+} band has been reduced enough to be measured as shown in Table III. It is not illustrated but is similar to the α-Fe^{3+} band in Figure 1 before any heat treatment although of somewhat lower absorbance.

Tables IV and V tabulate the absorption maxima of bands related to manganese that are too weak to be seen readily in the difference spectra of the whole rock;

TABLE IV

Chromic, titanous, manganic and manganus bands in zoned pyroxene from rock 12021.65

Ion	Probable structural position	Transition	Band maximum in eV	Absorbance	Δ cm^{-1}
Cr^{3+}	M_1	d-d	1.85	0.65	14920
Cr^{3+}	M_1	d-d	1.90	0.68	15325
Cr^{3+}	M_1	Charge transfer	3.95	2.02	31860
Ti^{3+}	M_1	Charge transfer	2.45	0.85	19760
Mn^{3+}	M_1	d-d	2.28	0.76	18390
Mn^{2+}	M_1	d-d	2.78	0.91	22425
Mn^{2+}	M_1	d-d	2.89	0.92	23310
Mn^{2+}	M_1	d-d	2.98	0.96	24035

TABLE V

Chromic, titanous, manganic and manganous bands in pyroxene
from rock 12018.50 after heating at 200–225°C for 2 h

Ion	Probable structural position	Transition	Band maximum in eV	Absorbance	Δ cm^{-1}
Cr^{3+}	M_1	d-d	1.80	0.62	14520
	M_1	d-d	1.89	0.64	15245
	M_1	d-d	2.01	0.66	16210
	M_1	Charge transfer	2.95	0.82	23795
	M_1	Charge transfer	3.9	1.29	31455
Ti^{3+}	M_1	Charge transfer	1.75	0.615	14115
	M_1	Charge transfer	2.45	0.735	19760
Mn^{3+}	M_1	d-d	2.28	0.68	18390
Mn^{2+}	M_1	d-d	2.95	0.81	23795

they are detectable in the spectra of the crystals of pyroxene and olivine. If the major portion of Fe^{3+} and Cr^{3+} are produced by oxidation of Fe^{2+} and Cr^{2+} respectively then the higher valence states which normally would favor M_1 positions may be in M_2 positions. The Fe^{3+} (3d^5) with zero crystal field stabilization energy would favor the M_1 site because of its smaller ionic size compared to Fe^{2+}. The Cr^{3+} (3d^5) ion would favor the M_1 sites both for crystal field and ionic size reasons. However Fe^{2+} (3d^6) and Cr^{2+} (3d^4) favor M_2 positions based on site distortion factors. Since the oxidized states are produced after the crystal has formed by radiation damage, one has Fe^{3+} in a Fe^{2+} site and Cr^{3+} in a Cr^{2+} site. These sites must undergo some local steric readjustment due to the change in cationic charge. The Ti^{4+} reduced to Ti^{3+} upon oxidation of the Fe^{2+} and Cr^{3+} may be in either silicon sites or M_1 sites or both, the M_1 site possibly being favored.

4. Spectra of Olivines in Rocks 12021 and 12018

The olivines in these two Apollo 12 rocks are the largest single crystals present. They are light yellow-green in color in 30 μ thickness. Figure 5 illustrates the Fe^{2+} spectrum of an olivine crystal in rock 12021.65 as found in the untreated rock and the spectrum of a single olivine crystal in rock 12018.50 after heating at 200–225 °C for two hours. Tables VI and VII tabulate the Fe^{2+} band data for these two crystals. The transitions are all *d-d* except the charge transfer bands near 2.0 eV. There is a Fe^{3+} charge transfer band in the ultraviolet region in the olivine crystal in rock 12021.65 at
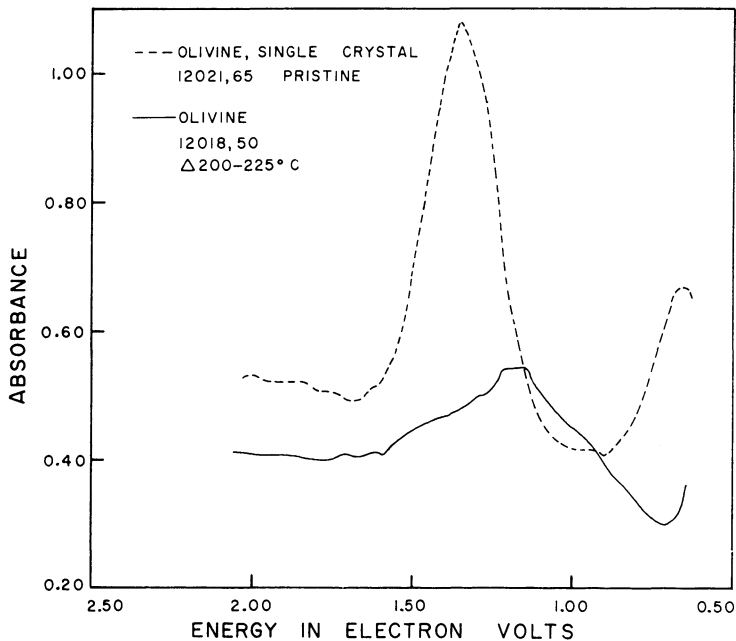

Fig. 5.

TABLE VI

Ferrous absorption band in olivine in rock 12021.65

Structural position	Band maximum in eV	Absorbance	Δ cm^{-1}
	0.66	0.68	5325
M_2	1.18	0.52	9520
M_1	1.34	1.08	10810
M_1	1.62	0.51	13065
Charge transfer $Fe^{2+} \to Fe^{3+}$	2.00	0.54	16130

TABLE VII

Ferrous absorption bands in olivine in rock 12018.50 after
heating at 200–225 °C for 2 h.

Structural position	Band maximum in eV	Absorbance	Δ cm^{-1}
M_2	1.18	0.54	9520
M_1	1.28	0.50	10325
M_1	1.62	0.41	13070
Charge transfer $Fe^{2+} \rightarrow Fe^{3+}$	2.05	0.38	16535

TABLE VIII

Chromic, titanous, manganic and manganous bands in olivine crystal in rock 12021.65

Ion	Probable structural position	Transition	Band maximum in eV	Absorbance	Δ cm^{-1}
Cr^{3+}	M_1	d-d	1.77	0.51	14275
Cr^{3+}	M_1	d-d	1.86	0.52	15000
Cr^{3+}	M_1	Charge transfer	4.00	1.67	32265
Cr^{3+}		Charge transfer	4.59	2.18	37020
Ti^{3+}	M_1	Charge transfer $Ti^{3+} \rightarrow Ti^{4+}$	2.44	0.645	19680
Mn^{3+}	M_1	d-d	2.30	0.58	18550
Mn^{2+}	M_1	d-d	2.67	0.67	21535

TABLE IX

Chromic, Titanous, Manganic and Manganous bands in olive crystal
in rock 12018.50 after heating at 200–225 °C for 2 h

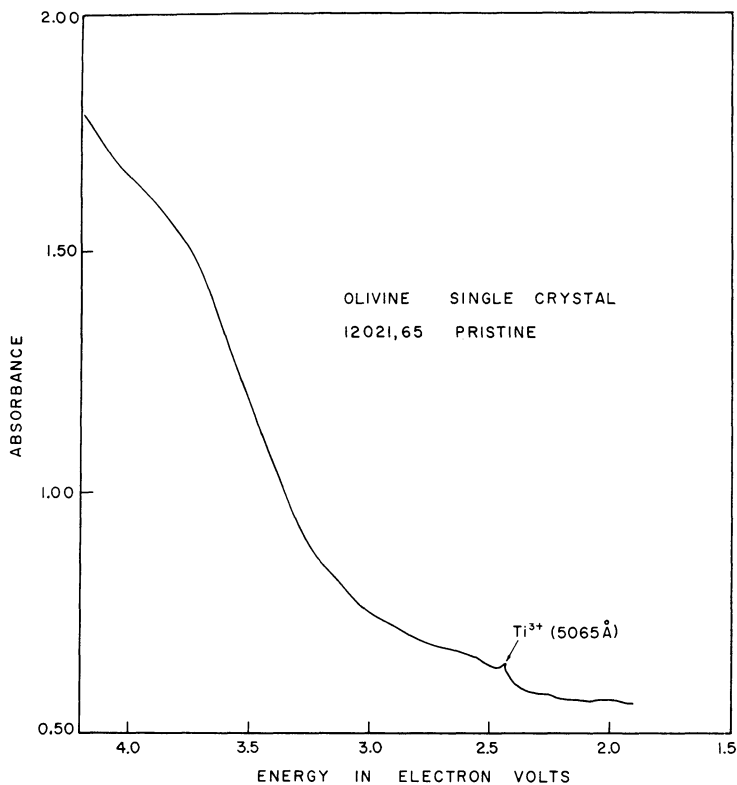| Ion	Probable structural position	Transition	Band maximum in eV	Absorbance	Δ cm^{-1}
Cr^{3+}	M_1	d-d	1.92	0.41	15485
Cr^{3+}		Charge transfer	3.24	0.55	26135
Cr^{3+}		Charge transfer	4.59	3.06	37020
Ti^{3+}	M_1	Charge transfer	1.71	0.41	13790
Ti^{3+}	M_1	Charge transfer $Ti^{3+} \rightarrow Ti^{4+}$	2.52	0.44	20325
Mn^{3+}	M_1	d-d	2.38	0.40	19195
Mn^{2+}	M_1	d-d	2.72	0.44	21940
Mn^{2+}	M_1	d-d	3.06	0.50	24680

274 ALVIN J. COHEN

Fig. 6.

5.64 eV with an absorbance of 2.86. The Fe^{3+} band was too intense to measure in the heated olivine from rock 12018.50.

The M_1 structural position in olivine is that of a tetragonally distorted octahedron while the M_2 site has the configuration of a trigonally distorted octahedron. The Fe^{2+} ion tends to favor the M_2 position in olivine.

Tables VIII and IX list the peaks of absorption bands attributed to Cr^{3+}, Ti^{3+}, Mn^{3+} and Mn^{2+} in the two olivines measured.

Figure 6 illustrates the high intensity of the Cr^{3+} charge-transfer band at 4.00 eV (3100A) compared to the Ti^{3+} charge transfer band in olivine at 2.44 eV (5065A). The Cr^{3+} band not shown at 4.59 eV is still more intense. This figure indicates that Cr^{3+} is important in affecting the color on the ultraviolet side of the spectrum as well as Fe^{3+} in both olivine and pyroxene.

5. Comparison of Difference Spectrum of Rock 12018.50 to Spectra of Pyroxene and Olivine

In Table X, the negative peaks in the difference spectrum of rock 12018.50 after heating at 200–225 °C for 2 h is compared to the spectra of the individual pyroxene

TABLE X

Mineral source of difference spectral bands in rock 12018.50

Ion	Rock peaks in eV (negative)	Pyroxene peaks in eV	Olivine peaks in eV
Fe^{2+}	1.28	1.31	1.28
Fe^{2+}	1.37	1.38	1.41
Ti^{3+}	1.72	1.75	1.71
Cr^{3+}	1.82	1.80	–
Cr^{3+}	1.94	1.94	1.92
Ti^{3+}	2.46	2.45	2.52
Mn^{2+}(?)	2.99	2.95	3.06
Cr^{3+}	3.20	–	–
Cr^{3+}	3.70	–	–
Cr^{3+}	4.06	3.9	–
Cr^{3+}	5.28	–	4.59
Fe^{3+}	5.90 (positive)	5.64	–
Mn^{2+}(?)	3.35	–	–
Mn^{2+}(?)	3.42	–	–

and olivine crystals in the same rock after heating. All peaks in the whole rock match peaks of either mineral or both minerals except the charge transfer peaks of Cr^{3+} (5.28) and Fe^{3+} (5.90) are shifted to higher energy. Also there is no Cr^{3+} peak at 3.7 in the minerals. The shift to higher energy in the deep ultraviolet may be apparent rather than real due to the increase of Ti^{4+} in the vacuum ultraviolet, the tail of which overlaps the Fe^{3+} and Cr^{3+} bands in the region 5–6 eV, causing them to appear to be at higher energy. This is caused by the increase in Ti^{4+} band due to oxidation of the Ti^{3+} on heating. The entire reaction on heating at 200–225°C appears to be:

$$Fe^{3+} + Cr^{3+} + 3Ti^{3+} (+Mn^{3+}) \rightarrow Fe^{2+} + Cr^{2+} + 3Ti^{4+} (+Mn^{2+}).$$
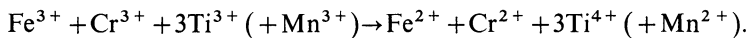
The data on Mn^{2+} is uncertain and the positive bands in the difference spectrum of the whole rock at 3.35 and 3.42 eV have not been positively identified.

6. Spectrum of Plagioclase in Rock 12021.65

The absorption spectrum of a single crystal of plagioclase in rock 12021.65 with dimensions 0.6 mm × 0.2 mm (× 30 μ thick) was measured. In the wavelength region 2000–17500 Å, there is no light absorption. The absence of the intense Fe^{3+} charge transfer band in the ultraviolet indicates that the Fe^{3+} ion in plagioclase is less than one ppm. The weakly absorbing Fe^{2+} could be present in the order of magnitude of 1000 ppm and not be detected. It is hoped to measure a thicker crystal of lunar plagioclase to see if any spectral bands can be observed.

7. The Absorption Spectrum of a Fragment of Oranges Glass in Brecciated Rock 10048.44

This 150 μ diam particle of orange glass in a polished section of breccia, 50 μ thick had the largest cross-section of any transparent material present. The glass fragment was roughly circular with a bright orange-red color in transmitted light. Figure 4 includes the spectrum of this glass in the visible region, the most prominent band is the $Fe^{2+} \rightarrow Fe^{3+}$ charge-transfer band with a maximum at 1.98 eV. Figure 7 shows
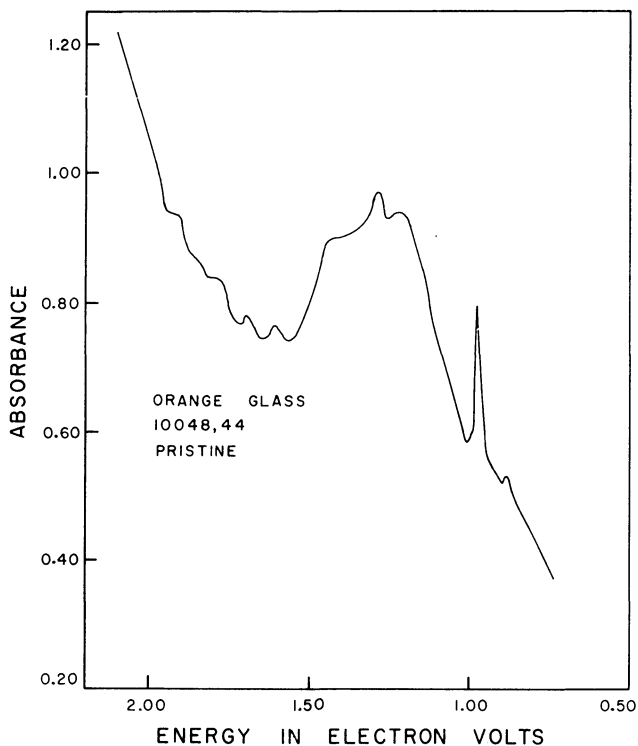

ORANGE GLASS
10048,44
PRISTINE

Fig. 7.

the absorption spectrum of the glass in the infra-red region. A prominent vibrational band is present at 0.98 eV. The source of this band has not been identified. Table XI lists the spectral bands present in this glass and the ions responsible. Due to the small size of the fragment, the spectrum could not be observed below 3.18 eV (3900A) because of its high intensity of absorption and the small amount of light transmitted by the small size of the fragment. Thus the ferric peak could not be observed although the 1.98 eV $Fe^{2+} \rightarrow Fe^{3+}$ charge-transfer band is present indicating that Fe^{3+} is present in the glass in sufficient quantity to interact with the Fe^{2+} ion.

TABLE XI

Absorption bands in orange glass fragment in brecciated rock 10048.44

Ion	Probable configuration	Transition	Band maximum in eV	Absorbance	Δ cm^{-1}
Fe^{2+}	octahedral	d-d	1.22	0.94	9840
Fe^{2+}	octahedral	d-d	1.29	0.97	10405
Fe^{2+}	octahedral	d-d	1.44	0.90	11615
Fe^{2+}	octahedral	d-d	1.61	0.77	12985
Fe^{2+}		Charge transfer	1.98	0.97	15970
Cr^{3+}	octahedral	d-d	1.80	0.84	14520
Cr^{3+}	octahedral	d-d	1.86	0.87	15000
Cr^{3+}	octahedral	d-d	1.93	0.94	15565
Ti^{3+}	octahedral	Charge transfer	1.69	0.78	13630
Ti^{3+}	octahedral	Charge transfer	2.48	1.52	20005
Mn^{3+}	octahedral	d-d	2.33	1.44	18795
Mn^{2+}	octahedral	d-d	2.18	1.33	10725
Mn^{2+}	octahedral	d-d	2.75	1.63	22180
Mn^{2+}	octahedral	d-d	2.85	1.67	22985
Mn^{2+}	octahedral	d-d	2.91	1.71	23390

7. Conclusions

Heating lunar basaltic rocks at low temperature in air causes reduction of Fe^{3+} and Cr^{3+} and oxidation of the Ti^{3+} in the pyroxenes and olivine present. It is probable that Mn^{3+} is present and reduced to Mn^{2+} by the mild heating at 200 to 225°C. It is suggested that Fe^{3+}, Cr^{3+}, and Mn^{3+} are reduced by such a mild heat treatment because they are not in equilibrium in the mineral structure. They are all in sites of the reduced species, viz. a Fe^{2+} site is the location of Fe^{3+} in the structure. The structural site must readjust to a smaller cation with different bonding. Electro-neutrality is preserved in the crystal by a Ti^{3+} being oxidized for each cation reduced by radiation. It is suggested that the most likely sources for the oxidation-reduction reactions are β-rays produced as secondaries following cosmic ray bombardment. Another source of β's is natural radioactivity present in the minerals. Since the rocks studied are from the interior of the rock, the effects of solar X-rays, ultraviolet light, and solar wind protons and electrons are negligible.

Absorption bands of Cr^{2+} were not detected in any of the specimens studied. Indications of Ti^{4+} were indicated by increase in the difference spectra of rocks in the deep ultraviolet upon oxidation of the Ti^{3+} present.

Deep-seated lunar rocks should be lower in Fe^{3+}, Cr^{3+}, and Ti^{3+} than surface rocks if the main source of the oxidation-reduction reactions is cosmic ray bombardment. The concentrations of these species should also increase with time of radiation by cosmic rays.

Acknowledgments

ALVIN J. COHEN

Space Administration. Mr Grover Moreland of the National Museum of Natural History, Washington, D.C., is thanked for preparation of the polished sections of lunar rock used in this work. Mr. Ed Skopinski prepared the final drawings of the figures.

Professor S. Keith Runcorn is thanked for the invitation to present this paper at the Moon Symposium at the University of Newcastle upon Tyne.

Note added in Proof: Olivine, single crystal in rocks 12021.65 should read: pigeonite, single crystal in rocks 12021.65, throughout the text, figures and tables.

References

Hapke, B. W., Cohen, A. J., Cassidy, W. A., and Wells, E. N.: 1970, 'Solar Radiation Effects on the Optical Properties of Apollo 11 Samples', *Proceedings of the Apollo 11 Lunar Science Conference*, 3, 2199, Pergamon Press.

Warner, J.: 1970, Apollo 12 Lunar-Sample Information NASA Technical Report R-353, p. 94–96.

Weeks, R. A., Kolopus, J. L., Kline D., and Chatelain, A.: 1970, 'Nuclear Resonance of ^{27}Al and Electron resonance of Fe and Mn', *Proceedings of the Apollo 11 Lunar Science Conference*, 3, 2467, Pergamon Press.